Environ. Sci. Technol. 1990, 24, 1528–1536

# Kinetics of Deposition of Colloidal Particles in Porous Media

**Menachem Elimelech*** **and Charles R. O'Melia†**

Civil Engineering Department, University of California, Los Angeles, California 90024, and Department of Geography and Environmental Engineering, The Johns Hopkins University, Baltimore, Maryland 21218

■ A theoretical framework for chemical–colloidal effects on the kinetics of deposition of Brownian particles in porous media has been presented. The theory was tested rigorously by conducting deposition experiments with model colloids and collectors under controlled chemical conditions in a well-defined experimental system. Experimental attachment (collision) efficiencies were calculated from measured particle deposition rates. The experimental results indicate that the attachment efficiencies are sensitive to the chemistry of the solution (electrolyte concentration and counterion type) but not to the large extent predicted by theory. A marked effect of particle size on attachment efficiencies is predicted by theory. Experimental attachment efficiencies, on the other hand, were virtually independent of particle size. DLVO theory is not successful in predicting the kinetics of deposition processes for Brownian particles flowing through porous media. Various explanations for the observed discrepancies are discussed.

## *Introduction*

The rate of deposition of colloids from flowing suspensions onto solid surfaces (collectors) determines the kinetics of many technological and natural processes. Examples include (i) granular (deep-bed) filtration in water and wastewater treatment and in industrial applications, (ii) transport and fate of colloids and colloid-associated pollutants in subsurface environments, (iii) fouling of membranes and heat exchangers by colloidal particles, and (iv) release and redeposition of corrosion products. Deposition can also be used as a means of investigating colloidal phenomena. By studying the deposition of model colloids on well-defined solid surfaces, various theoretical aspects of colloidal interactions can be tested.

The process of deposition is conveniently divided into two sequential steps: *transport* and *attachment*. In the first step the particles are transported from the bulk of the fluid to the vicinity of a stationary surface. Transport of Brownian (submicron) particles is dominated by convection and diffusion, while that of larger (non-Brownian) particles is controlled by physical forces arising from gravity and fluid drag and by interception due to the finite size of the particles (*1*, *2*). Transport models for several surface geometries have been established and validated experimentally (*1*, *3–6*). Attachment, on the other hand, is dominated by the various chemical–colloidal interactions that act between particles and surfaces at short distances. These colloidal interactions include electrical double layer and van der Waals interactions, hydrodynamic interactions, hydration (structural) forces, hydrophobic interactions for hydrophobic surfaces, and macromolecular adsorbed layer (*steric*) interactions when macromolecules or polymers are adsorbed onto the interfaces of interacting particles and surfaces. The overall kinetics of particle deposition are determined by the rates of particle transport and attachment.

The kinetics of capture (attachment) of colloids are determined by the magnitude of the colloidal interactions between particles and collectors. These, in turn, are controlled by the chemical characteristics of the solid–solution interface of colloids and collectors and by the solution chemistry. The critical role of solution chemistry and colloidal interactions in the attachment step is poorly understood (*7–10*). The objectives of this paper are (i) to present a theoretical framework for the effects of chemical–colloidal interactions on the attachment efficiency in the deposition of Brownian particles in porous media and (ii) to test the theory by conducting deposition experiments with model colloids and collectors in a well-defined experimental system under controlled chemical conditions.

## *Theoretical Approach*

The theoretical approach for investigating chemical–colloidal effects on the attachment step in deposition combines fundamental theories of mass transfer in porous media, physicochemical hydrodynamics, and colloidal stability and interaction. A brief description of the theory is given below. A detailed description of this approach was presented elsewhere (*11*).

**Transport of Brownian Particles.** The governing equation for the concentration distribution of Brownian particles over a surface in the presence of interaction forces is (*2*, *12*)

$$\frac{\partial C}{\partial t} + \vec{v}\cdot\nabla C = \nabla\cdot(D\nabla C + mC\nabla\Phi) \qquad (1)$$

where $C$ is the particle number concentration, $t$ is the time, $\vec{v}$ is the particle velocity vector, $D$ is the position-dependent diffusion coefficient, $m$ is the particle mobility, and $\Phi$ is the total colloidal interaction energy. This equation in its general form is commonly referred to as the *transport equation* or the *convective diffusion equation.*

The position-dependent diffusion coefficient ($D$) and the particle mobility ($m$) can be obtained from the diffusion coefficient at infinite separation. Corrections for the retardation in the mobility of colloids at short distances from a collector due to hydrodynamic interactions have to be made (*13–16*). The diffusion coefficient at infinite separation can be found from the *Stokes–Einstein* equation (*1*, *12*, *16*). The fluid velocity components are derived from the stream function around a spherical collector (*17*). The latter is obtained from the solution of the *Navier–Stokes* equation under the assumptions of steady and low Reynolds number flow. Happel's (*18*) porous medium model is used to account for the disturbance of the flow field around a spherical collector by neighboring collectors.

**Colloidal Interactions.** Colloidal interactions play a significant role when a particle approaches a collector at short distances (several to a few tens of nanometers) during the attachment step in deposition. In the DLVO theory of colloid stability (*19*, *20*), the total interaction energy as a function of separation distance is considered as the sum of van der Waals and electric double layer interactions. In deposition of Brownian particles the particles are much smaller than the collectors, and as a result, theoretical expressions for interaction energy between a sphere and a planar surface can be used.

Van der Waals interaction forces depend on the size (diameter) of the interacting particles, the distance of

* University of California.
† The Johns Hopkins University.

 0013-936X/90/0924-1528$02.50/0 

separation between particles and collector, and the Hamaker constant of the interacting media. Analytical expressions for these interactions are available in the literature (*21–23*). The expression derived by Gregory (*23*) has been used in the theoretical computations of this work.

The magnitude of the electrical double layer repulsion between similarly charged surfaces depends on the size of the interacting particles, the distance of separation, the surface potential of particles and collectors, and the electrolyte concentration and counterion valence. Quantitative theories for these interactions are available in the literature (*20, 24, 25*). The expression derived by Hogg et al. (*24*) for interaction at constant potential has been used in this work.

**Kinetics of Deposition.** In studies of deposition of colloidal particles onto collector surfaces it is useful to express rates of particle deposition in a dimensionless form. A common approach is the use of the so called *single collector efficiency* (*1, 26*). It is defined as the ratio of the total particle deposition rate on the collector to the rate at which particles approach the projected area of the collector from the upstream.

The dimensionless deposition (or removal) rate of particles ($\eta_R$) can be viewed as a product of an attachment efficiency ($\alpha$) and a dimensionless transport rate ($\eta_T$):

$$\eta_R = \alpha\eta_T \tag{2}$$

The attachment efficiency ($\alpha$) accounts for chemical–colloidal effects on the rate of deposition, while $\eta_T$ accounts for physical effects (*8*). Thus, when chemical–colloidal interactions are favorable for deposition (i.e., in the absence of repulsive total interaction energies), the attachment efficiency approaches unity, and the deposition rate is equal to the transport rate. In this case particle transport is the rate-determining step; this case is generally referred to as *favorable deposition*. When chemical–colloidal interactions are unfavorable for deposition (i.e., repulsive colloidal interactions predominate), the attachment efficiency is smaller than one and particle deposition rates are hindered. This case is referred to as *unfavorable deposition*.

The dimensionless particle deposition and transport rates, $\eta_R$ and $\eta_T$, respectively, can be evaluated from the solution of the transport equation. Levich (*27*) solved the transport equation analytically for the concentration distribution and deposition rate on a spherical collector. In his solution colloidal and hydrodynamic interactions were not included. In this case the deposition rate is equal to the transport rate. The analytical expression of Levich (*27*) for the transport rate can be expressed in terms of a dimensionless single collector transport efficiency ($\eta_T$) as follows (*1*):

$$\eta_T = 4.0A_s^{1/3}Pe^{-2/3} \tag{3}$$

where $A_s$ is a porosity-dependent parameter of Happel's (*18*) porous medium model, and Pe is a dimensionless Peclet number defined as $2a_cU/D_\infty$; $a_c$ is the diameter of the sperical collector, $U$ is the approach velocity of the fluid toward the collector, and $D_\infty$ is the diffusion coefficient at infinite separation.

An approximate analytical solution for the dimensionless deposition rate (or the single collector removal efficiency $\eta_R$), in the presence of electrical double layer repulsion and van der Waals attraction, was derived by Spielman and Friedlander (*12*). This equation was later modified by Dahneke to partially include hydrodynamic interactions. A theoretical expression for the attachment efficiency ($\alpha_{the}$) can be obtained from the ratio of $\eta_R$, as obtained by Spielman and Friedlander (*12*), and $\eta_T$ (eq 3):

$$\alpha_{the} = \left(\frac{\beta}{1+\beta}\right)S(\beta) \tag{4}$$

where $\beta$ is an analytical expression that depends on the total colloidal interaction energy (*11, 12*) and $S(\beta)$ is a slowly varying function of $\beta$ with tabulated values given in Spielman and Friedlander (*12*). Further analysis (*11*) shows that the attachment efficiency is proportional to $\exp(-|\Phi/kT|)$, where $k$ is the Boltzmann's constant and $T$ is the absolute temperature. The ratio $\Phi/kT$ is a dimensionless form of the total interaction energy. This relation indicates that theoretical attachment efficiencies are very sensitive to the total interaction energy $\Phi$. This, in turn, is determined by the solution chemistry and by the chemical characteristics of the solid–solution interfaces.

**Chemical–Colloidal Effects on the Attachment Efficiency.** The effects of solution chemistry and colloidal interactions on the attachment efficiency can be predicted by the theoretical framework developed. Theoretical computations show the following relation:

$$\frac{\mathrm{d}\log\alpha_{the}}{\mathrm{d}\log C_s} = -B(\psi_p,\psi_c,z)a_p \tag{5}$$

in which $C_s$ is the electrolyte concentration, $B$ is a numerically evaluated function that depends on the surface potentials of particles and collectors ($\psi_p$ and $\psi_c$, respectively) and the valence of the counterions ($z$), and $a_p$ is the radius of the suspended colloids. As shown by eq 5 the slope of $\log\alpha_{the} - \log C_s$ curves is sensitive to $\psi_p$, $\psi_c$, $z$, and $a_p$. With this framework, theoretical predictions can be compared to experimental results. A unique feature of this relation is the dependence of the attachment efficiency on the diameter of suspended colloids. Theory predicts a linear dependence of the slope of $\log\alpha_{the} - \log C_s$ curves on particle size (radius).

## *Experimental Section*

**Model Colloids.** Surfactant-free polystyrene latex particles with sulfate functional groups (manufactured by Interfacial Dynamics Corp., Portland, OR) were used as model colloids. The particles are spherical and monodisperse and have comparable chemical properties. Three different sizes (0.046, 0.378, and 0.753 μm in diameter) were utilized. The colloids were extensively dialyzed by the manufacturer to remove trace impurities.

**Model Collectors.** Spherical glass beads (0.2 and 0.4 mm in diameter) were used as model collectors for deposition studies (manufactured by Ferro Corp., Jackson, MS). The glass beads were cleaned with a 1 M $HNO_3$. Then they were rinsed with distilled deionized water and dried in an oven at 60 °C. The collectors were packed in a cylindrical Plexiglass column to a porosity of 0.4. Scanning electron micrographs indicate that the collectors are spherical and relatively smooth.

**Solution Chemistry.** KCl and $CaCl_2$ salts were used as destabilizing electrolytes. Inorganic salts were analytical reagent grade and water was distilled deionized (Milli-Q system, Millipore Corp., Bedford, MA). Salt concentrations were varied over a wide range (0.001–0.3 M) so that favorable and unfavorable deposition can be studied. The pH of the colloidal suspensions used in the deposition studies was adjusted to 6.7 by adding $NaHCO_3$ ($5 \times 10^{-5}$ M).

**Surface Characterization.** Conductometric and potentiometric (acid–base) titrations were used to characterize the surface charge properties of the model colloids. The procedure developed by Van den Hul and Vanderhoff (*28*) for such titrations was utilized. Latex particles were

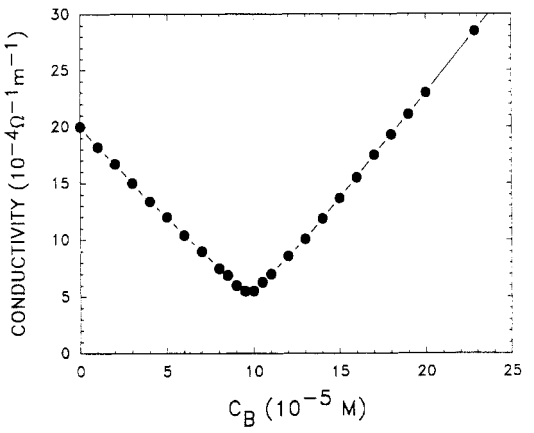


**Figure 1.** Representative conductometric titration curve of latex colloids (particle size 0.046 μm, solid concentraion 2.0 g/L, temperature 25 °C). The measured conductivity is presented as a function of base concentration ($C_B$) after the addition of NaOH to the titration vessel. The particles were suspended in distilled deionized water.

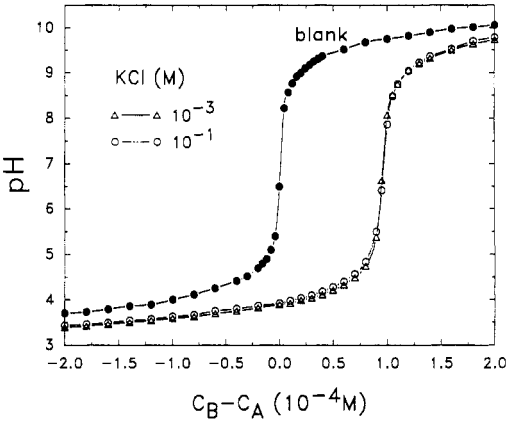


**Figure 2.** Representative potentiometric (acid–base) titration curves of latex colloids at different ionic strengths (particle size 0.046 μm, solid concentration 2.0 g/L, temperature 25 °C). $C_B - C_A$ is the excess of base ($C_B$) or acid ($C_A$) added. Particles were suspended in distilled deionized water.

ion exchanged prior to titration studies (performed by the manufacturer). Electrophoretic mobilities of the latex particles and glass microspheres with average size of ~5 μm were determined by microelectrophoresis (Mark II, Rank Brothers, Cambridge, UK). The glass microspheres had a chemical composition similar to the glass bead collectors (produced by the same manufacturer). The pH of the solutions in these measurements was adjusted to 6.7 by adding $NaHCO_3$ ($5 \times 10^{-5}$ M). The temperature of the suspensions in the titration and electrophoretic mobility experiments was constant at 25 °C.

**Deposition Experiments.** Latex particles were suspended in distilled deionized water. Dilute suspensions of particles (1–4 mg/L) were used in the deposition studies. Suspensions were pumped through the packed-bed column at a constant flow rate, producing an approach velocity of 0.14 cm/s. A proper dose of a destabilizing electrolyte was applied to the influent by a peristaltic pump. The electrolyte was applied just ahead of the packed column in order to prevent aggregation prior to deposition. Deposition experiments were carried out under chemical conditions similar to those used in the electrophoretic mobility measurements. The pH in the effluent suspension ranged from 6.8 to 7.2 and the temperature was between 23 and 25 °C. Samples of effluent suspension were taken at short time intervals. Particle concentrations of the samples were determined by light extinction (optical density) measurements using a Perkin-Elmer spectrophotometer, Model Lambda 3).

*Results and Discussion*

**Electrokinetic Properties of Colloids and Collectors.** Conductometric and potentiometric titrations were carried out in order to find the surface charge density of the model colloids and the type of the surface functional groups. A representative conductometric titration curve is shown in Figure 1. The shape of the conductometric titration curve indicates that the latex particles have strong acid functional groups (*29*, *30*). These are sulfate functional groups ($OSO_3H$) with a $pK_a$ of ~2 (*30*). The absence of weak acid groups is also demonstrated in Figure 2 in which the results of potentiometric (acid–base) titrations conducted at different ionic strengths are presented. The curves at different ionic strengths are identical and have the same shape as that of the blank titration curve. This behavior indicates that the surface sites are strong acids that are fully dissociated over the pH range employed in the titrations (*29–31*). The charge densities of the latex

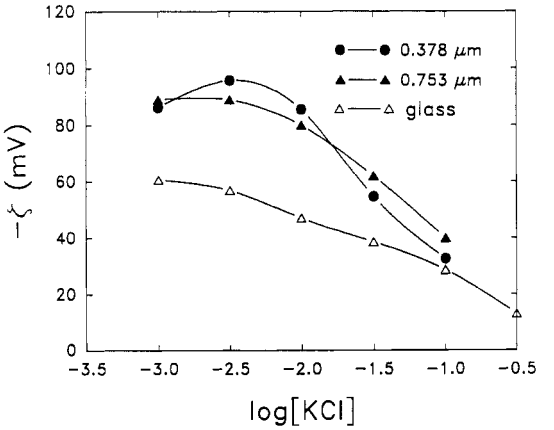


**Figure 3.** ζ potentials of latex colloids and glass beads as a function of log-molar KCl concentration (pH 6.7). The ζ potentials were calculated from the measured average electrophoretic mobilities.

particles as determined by conductometric titrations are 3.90, 4.25, and 5.64 μC/cm² for the 0.046, 0.378, and 0.753-μm suspensions, respectively.

ζ potentials were calculated from the measured mean electrophoretic mobilities by using the tabulated numerical calculations of Ottewill and Shaw (*32*). These calculations consider corrections for the retardation and relaxation effects. The ζ potential of the colloids and glass microspheres as a function of KCl concentrations are presented in Figure 3. As observed, the ζ potentials of the model colloids and collectors decrease with increasing KCl concentrations. The ζ potential of the latex particles is much higher (more negative) than that of the glass bead collectors at low electrolyte concentrations and becomes comparable at high electrolyte concentration (0.1 M KCl). The anomalous maximum observed with the 0.378-μm latex particles (at ~$10^{-2.5}$ M KCl) is a common feature of polystyrene latex colloids with sulfate functional groups and was discussed in detail elsewhere (*33*).

The ζ potentials of the latex particles and collectors as a function of $CaCl_2$ concentration, in the presence of 0.01 M KCl, are described in Figure 4. In the presence of 0.01 M KCl as a background electrolyte the ζ potentials decrease continuously with increasing $CaCl_2$ concentrations. The absolute values of the ζ potentials with $CaCl_2$ are smaller than those with KCl. This is attributed to the higher ionic strength in the experiments with $CaCl_2$ and probably also due to some specific interaction of $Ca^{2+}$ at the surface of colloids and collectors. The apparent specific

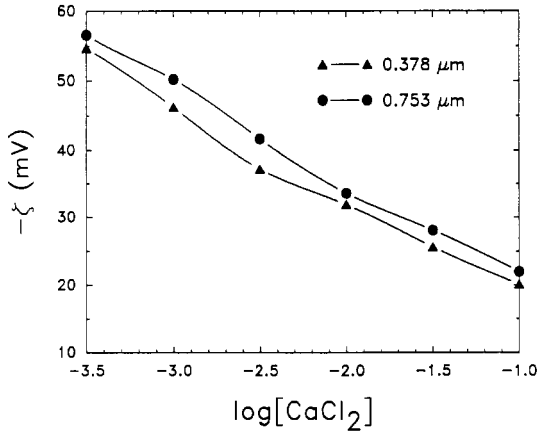


**Figure 4.** $\zeta$ potentials of latex colloids as a function of log-molar $CaCl_2$ concentration in the presence of 0.01 M KCl as a background electrolyte (pH 6.7). The $\zeta$ potentials were calculated from the measured average electrophoretic mobilities.

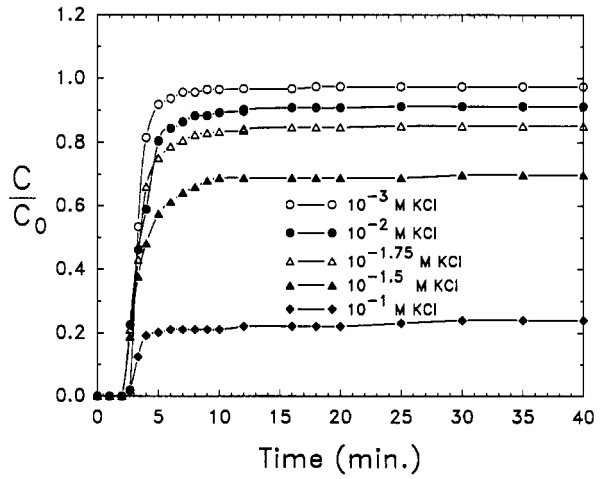


**Figure 5.** Particle breakthrough curves of the 0.753-$\mu$m latex particles with various concentrations of KCl. The residual particle concentration $C/C_0$ is plotted as a function of time. Experimental conditions were as follows: approach velocity 0.14 cm/s, bed depth 20 cm, collector size 0.2 mm.

interaction is not strong since no reversal of charge was observed at high $CaCl_2$ concentrations.

Due to the small size of the 0.046-$\mu$m latex colloids and the low refractive index of polystyrene it was not possible to measure the mobility of these particles by microelectrophoresis, even with the use of laser illumination. It was therefore assumed that the $\zeta$ potentials of these particles are equal to those of the 0.378-$\mu$m particles. This is a reasonable assumption since the charge densities and the surface properties of these suspensions are comparable.

**Particle Breakthrough Curves.** Deposition experiments with chemical conditions similar to those employed in the electrophoretic mobility measurements were conducted. The results are presented as breakthrough curves, i.e., the fraction of the influent particle concentration leaving the packed bed, $C/C_0$, as a function of time ($C$ and $C_0$ are the effluent and influent concentrations of colloids, respectively). Due to the large amount of experimental data obtained, only representative breakthrough curves illustrating the various features of the deposition experiments will be presented.

Typical particle breakthrough curves at different KCl concentrations are presented in Figure 5. The shape of the particle breakthrough curves when there is no significant removal of particles ($C/C_0$ close to 1) is similar to that of breakthrough curves of an inert tracer obtained in this work (*11*). The characteristic sigmoidal shape of the breakthrough curves is caused by dispersion of the colloidal particles in the packed bed and the inlet and outlet sections of the column, as in the case of inert tracer molecules.

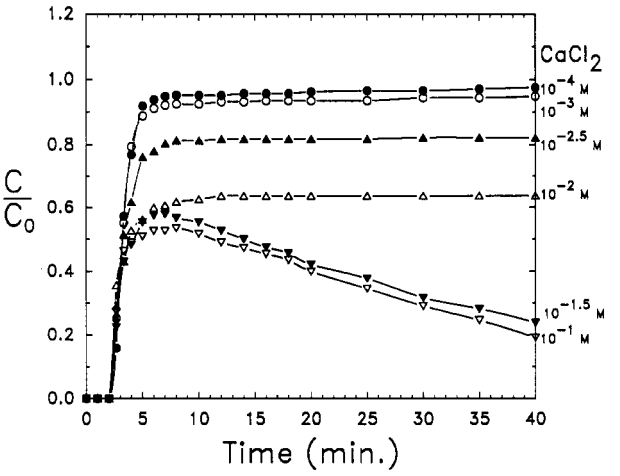


**Figure 6.** Particle breakthrough curves of the 0.753-$\mu$m latex particles with various concentrations of $CaCl_2$ in the presence of 0.01 M KCl. The residual particle concentration $C/C_0$ is plotted as a function of time. Experimental conditions were as follows: approach velocity 0.14 cm/s, bed depth 20 cm, collector size 0.4 mm.

As observed in Figure 5, particle deposition rates (or removal efficiencies) increase ($C/C_0$ values decrease) with increasing KCl concentrations, when the physical conditions are similar. This finding is in qualitative agreement with the DLVO theory. As the concentration of KCl in the solution increases the diffuse double layers are compressed, the $\zeta$ potentials decrease (less negative), and the electrical double layer repulsions are reduced. Since the attractive van der Waals interaction is independent of the solution chemistry, the total interaction energy and the height of the energy barrier decrease, and as a result, the deposition rates increase. At very low salt concentrations, the repulsive electrical double layer interactions are very large and the removal of particles is very low ($C/C_0$ close to 1).

Deposition experiments were also carried out with various concentrations of $CaCl_2$ in the presence of 0.01 M KCl as a background electrolyte. As discussed earlier, in the presence of 0.01 M KCl, the electrokinetic potential of the latex particles decreases continuously with increasing $CaCl_2$ concentration so that these particles can be used as model colloids to study chemical–colloidal aspects in deposition. The effect of solution chemistry on the deposition of particles is illustrated in Figure 6 in which residual particle concentrations, $C/C_0$, as a function of time for various $CaCl_2$ concentrations are described. As in the case with KCl (Figure 5), the removal of particles increases with increasing $CaCl_2$ concentration due to reduced electrical double layer repulsion energies. Bivalent electrolytes such as $CaCl_2$ can interact specifically with the surface of particles and collectors and cause a marked decrease in the electrokinetic potentials and the electrical double layer repulsion energies.

A noticeable increase in particle removal with time is observed at high $CaCl_2$ concentrations ($10^{-1.5}$ and $10^{-1}$ M). A similar effect has been reported by Tobiason and O'Melia (*9*) for deposition of non-Brownian latex particles on glass beads with $CaCl_2$. This phenomenon was also observed in filtration studies with polyelectrolytes as destabilizing chemicals and is commonly referred to as *filter ripening* (*1*, *34*). The improvement in particle removal with time may indicate that the interaction between approaching particles and particles that had been already

deposited is more favorable (for deposition) than the interaction of the approaching particles with the bare collectors. The ripening process starts before the time corresponding to a complete breakthrough of an inert tracer. For the deposition experiments described in Figure 6, ripening starts at ~8 min while complete breakthrough curves occur at 12 min. This indicates that a relatively small number of retained particles that are destabilized can improve the deposition rate significantly.

**Experimental Attachment Efficiencies.** For a given suspension, the removal of particles as obtained from the particle breakthrough curves depends on the solution chemistry of the suspension and on physical parameters such as the approach velocity, media depth and size, and bed porosity. Since this work focuses on the effect of solution chemistry and colloidal interactions on the kinetics of particle deposition, it is necessary that experimental attachment efficiencies be calculated from the results of the deposition experiments. The attachment efficiency, as defined previously under Theoretical Approach, depends on the colloidal interactions between particles and collectors; it approaches unity when colloidal interactions are favorable for deposition and is much smaller than 1 when the colloidal interactions are unfavorable for deposition. Experimental attachment efficiencies (will be denoted as $\alpha_{exp}$) can be plotted as stability curves, i.e., log $\alpha_{exp}$ against log $C_s$. These curves can be compared to theoretical stability curves according to the procedure described under Theoretical Approach.

By performing a mass balance of particles over a differential packed-bed volume and integrating over the entire bed depth, an expression that relates the experimental attachment efficiency, $\alpha_{exp}$, to the initial (clean-bed) removal, $(C/C_0)_0$, can be obtained (*35*):

$$\alpha_{exp} = -\ln (C/C_0)_0 \left( \frac{4a_c}{3(1-\epsilon)L\eta_T} \right) \qquad (6)$$

where $\epsilon$ is the porosity of the bed, $L$ is the media depth, and $a_c$ is the collector radius. The clean bed removal efficiency, $(C/C_0)_0$, is determined from the particle breakthrough curves. This is the value of $C/C_0$ at a time correspondng to a complete breakthrough curve of an inert tracer. The time of the clean bed removals for the physical conditions of the breakthrough curves described in Figures 5 and 6 was found to be 12 min.

Experimental attachment efficiencies were determined by following the procedure described earlier. The results are presented as stability curves, i.e., the logarithm of $\alpha_{exp}$ as a function of the logarithm of molar electrolyte concentration. Average values of $\alpha_{exp}$ were used when more than one experiment at a given electrolyte concentration was performed. The experimental stability curves with KCl and $CaCl_2$ are described below.

Experimental stability curves for the three colloidal suspensions with KCl as a destabilizing electrolyte are presented in Figure 7. The results are presented for KCl concentrations larger than $10^{-2.5}$ M. A gradual increase in the attachment efficiency with increasing KCl concentration is observed. As the electrolyte concentrations increase, the energy barrier is reduced, and as a result, the fraction of particle collisions that are "successful" in making attachment is increased. At the KCl concentration range of $10^{-1}$–$10^{-0.5}$ M the attachment efficiencies do not change significantly with increasing KCl concentration. The variation of the slopes with particle size as expected from theory (eq 5) was not observed. As shown, the slopes of all the curves are remarkably similar, despite the fact that the particle diameters varied by more than 1 order of

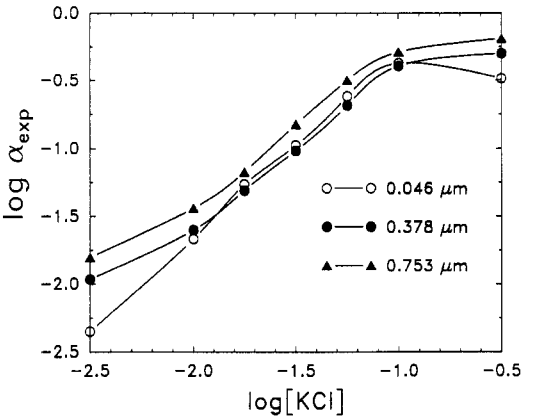


**Figure 7.** Experimental stability curves of the model colloids. The logarithm of the experimental attachment efficiencies is plotted as a function of the logarithm of molar KCl concentrations.

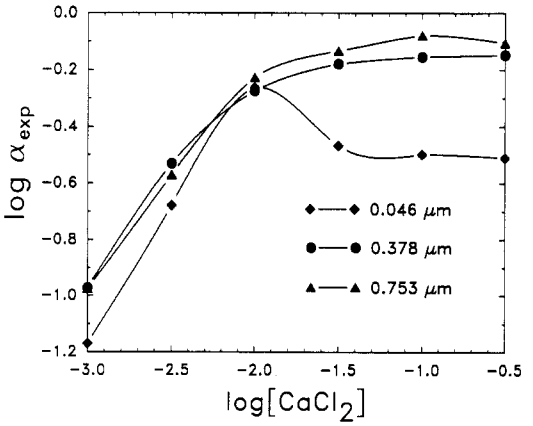


**Figure 8.** Experimental stability curves of the model colloids. The logarithm of the experimental attachment efficiencies is plotted as a function of the logarithm of molar $CaCl_2$ concentrations in the presence of 0.01 M KCl.

magnitude. Attachment efficiencies increased by almost 2 orders of magnitude when the electrolyte concentration varied from $10^{-2.5}$ to $10^{-1}$ M, indicating the importance of chemical–colloidal aspects in the kinetics of particle deposition.

Similar observations were found in the stability curves with $CaCl_2$ as a destabilizing electrolyte. The experimental stability curves with $CaCl_2$ as calculated from the corresponding breakthrough curves are presented in Figure 8. The attachment efficiencies increase gradually with $CaCl_2$ up to ~0.01 M; then they remain constant. As expected, the attachment efficiencies are larger than those obtained with KCl. This is because the ionic strength and the valence of the counterions are higher than those with KCl. The values of the attachment efficiencies and the slopes of the stability curves of all suspensions are comparable. This is in a marked contrast to theory, which predicts larger slopes with increasing particle size (eq 5). The maximum in the stability curve of the 0.046-μm particles and the observation that the attachment efficiencies at high electrolyte concentrations (with KCl and $CaCl_2$) are smaller than 1 will be discussed subsequently in this paper.

**Theoretical Predictions.** The theoretical evaluation of the attachment efficiencies and stability curves (eq 4 and 5) involves the determination of van der Waals and electrical double layer interactions. In order to calculate the van der Waals attraction for the polystyrene–water–glass interacting media, a suitable value of the Hamaker constant is needed. A value of $1 \times 10^{-20}$ J for similar interacting media was calculated by Spielman and FitzPatrick (*36*) from the Hamaker constants of glass

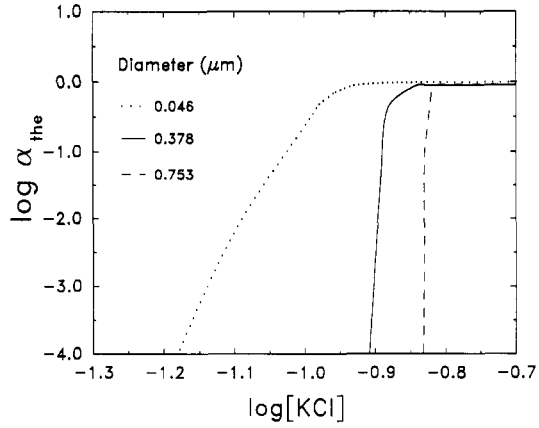


**Figure 9.** Theoretical stability curves of the model colloids employed in this research. The following parameters were used: KCl concentration in molar, surface potentials of particles and collectors were replaced by the measured mean $\zeta$ potentials, approach velocity 0.14 cm/s, porosity 0.4, collector diameter 0.2 mm, temperature 24 °C.

($SiO_2$) and polystyrene using the Hamaker approach (*22*). A similar value for the polystyrene–water–glass mdeia was utilized by Yoshimura et al. (*37*) and Tobiason and O'Melia (*9*). It was therefore decided to use this value for the Hamaker constant in this work. The equation derived by Gregory (*23*) for the van der Waals interaction, which includes correction for electromagnetic retardation, was used.

In order to calculate electrical double layer repulsion, proper values for the surface potentials are required. Since electrical double layer interaction arises from the overlapping of diffuse double layers, the surface potentials can be represented by the potential at the boundary between the Stern and diffuse layers (the so-called "*Stern potential*" or "*diffuse layer potential*"). This potential cannot be measured directly, and the electrokinetic ($\zeta$) potential is usually considered as a good approximation (*38*). $\zeta$ potentials measured in this work were used in the constant surface potential interaction expression of Hogg et al. (*24*) to calculate electrical double layer repulsion.

The theoretical stability curves of the latex colloids investigated are presented in Figure 9. Since the evaluation of electrical double layer interactions with the framework of the DLVO theory is valid only for 1:1 electrolytes (*24, 39*), the theoretical predictions in this work were carried out only for the stability curves with KCl. The mean $\zeta$ potentials of particles and collectors at a given KCl concentration were used as surface potentials in electrical double layer interaction calculations. A common feature of the curves, as was also found in other studies (*10, 40, 41*), is the drastic drop of the attachment efficiency practically to zero below a certain electrolyte concentration. This electrolyte concentration demarcates the transition from favorable to unfavorable deposition and will be referred to as the *critical deposition concentration*. Above the critical deposition concentration $\alpha = 1$; this means that each collision between particles and collectors results in attachment. The theoretical predictions indicate that the colloidal stability of the particles increases with particle size. This is evidenced by the larger slopes of the log $\alpha$ – log $C_s$ curves and the higher critical deposition concentrations for larger particles.

As mentioned previously, theoretical predictions indicate that the logarithm of the attachment efficiency is approximately proportional to the height of the energy barrier. This is confirmed by the results shown in Figure 10 in which the logarithm of the attachment efficiency of the 0.046-μm particles as a function of the height of the

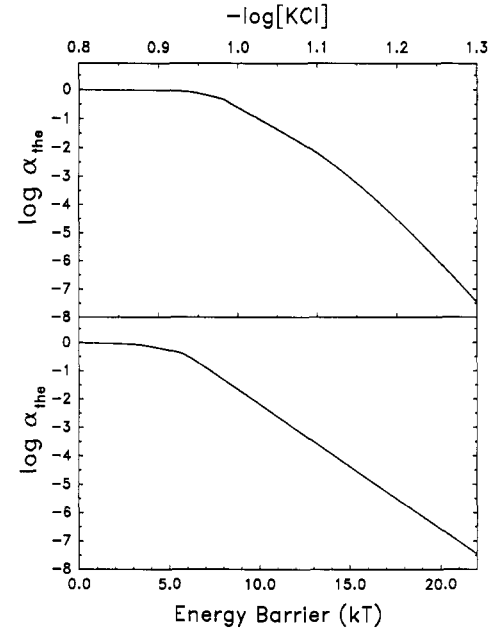


**Figure 10.** Theoretical attachment efficiencies of the 0.046-μm suspension as a function of molar salt concentration and the calculated energy barrier at these chemical conditions.

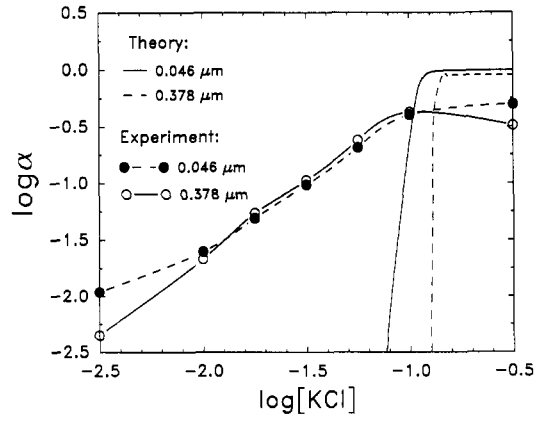


**Figure 11.** Comparison of theoretical and experimental stability curves of the 0.046- and 0.378-μm suspensions.

energy barrier and the log molar KCl concentration is presented. The $\zeta$ potentials at the corresponding KCl concentrations were taken as the surface potentials in the calculations of the total interaction energy. As shown, the transition from favorable to unfavorable deposition is at an energy barrier of ~5 kT. This type of presentation is very useful since the attachment efficiency is dependent on the salt concentration, which in turn determines the height of the energy barrier.

**Theory and Observations.** Theoretical and experimental stability curves of the 0.046- and 0.378-μm suspensions are presented in Figure 11. It is demonstrated that the experimental curves are in marked contrast with theory. The slopes of the experimental stability curves and the critical deposition concentrations are independent of particle size while model predictions are sensitive to the size of the particles. Also, the experimental attachment efficiencies decrease gradually with decreasing KCl concentration whereas theoretical values decrease sharply. The disagreement between observations and theory increases markedly with increasing particle size as a result of the higher energy barriers predicted for larger particles.

At electrolyte concentrations higher than the critical deposition concentration, the experimental attachment efficiencies are smaller than the theoretical values, which

approach unity. This discrepancy may be attributed to the procedure used to calculate $\alpha_{exp}$ (eq 6). In this equation $\alpha_{exp}$ is calculated from the ratio of the experimental single collector efficiency to the theoretical dimensionless transport rate $\eta_T$ (eq 3). The latter may overestimate the real value since hydrodynamic interactions were not included in its derivation. As a result, experimental attachment efficiencies smaller than unity can be obtained. A similar explanation was suggested by Gregory and Wishart (*38*), who obtained $\alpha_{exp}$ values smaller than 1 for deposition in the absence of energy barriers. It is also possible that the porosity-dependent parameter ($A_s$) used in eq 3 overestimates the effect of neighboring collectors.

Another possible explanation for the fact that $\alpha_{exp}$ is smaller than unity in favorable deposition is the existence of hydration forces (also referred to as structural or solvation forces) at high ionic strengths. The origin of these short-range forces is primarily due to hydration of surface functional groups and counterions at the interface (*42*). Some indirect evidence for the presence of repulsive hydration forces at high ionic strengths can be found in the stability curves of the 0.046-$\mu$m latex particles in which a maximum in the attachment efficiency is observed. It was found that the experimental attachment efficiency exhibits a maximum at $\sim$0.01 M $CaCl_2$ (Figure 8). At $CaCl_2$ concentrations larger than 0.01 M the attachment efficiency decreased, indicating an apparent increase of repulsion with salt concentration. A similar but less pronounced observation was found with KCl where $\alpha_{exp}$ of the 0.046-$\mu$m particles decreased with increasing KCl concentration from $10^{-1}$ to $10^{-0.5}$ M (Figure 7). This subject was discussed in more detail elsewhere (*43*).

**Possible Explanations for Observed Discrepancies.** Two major discrepancies between theory and observations were described. These are as follows: (i) experimental attachment efficiencies were orders of magnitude larger than predicted values in the unfavorable deposition region, and (ii) experimental attachment efficiencies and critical deposition concentrations were independent of particle size. Both of these discrepancies are probably related to the inadequacy of the DLVO theory to describe quantitatively the total interaction energy during particle–collector interactions (*11*). When repulsive forces are absent (favorable deposition), theoretical predictions differ from experimental results by no more than a factor of 2.

Several explanations for the poor agreement between theory and observations with regard to the magnitude of the attachment efficiency were proposed in the past two decades. Among the explanations are surface roughness of particles and collectors, heterogeneity of surface charge, and interfacial electrodynamics of double layers during interaction (*7*, *45–47*). However, no quantitative theory to resolve this discrepancy is available.

The contradiction between theory and experiments with regard to particle size effects can be attributed to several factors. These include (i) hydrodynamic interaction, (ii) a distribution in surface potentials of interacting media, (iii) dynamics of interaction, (iv) deposition in secondary minima, and (v) surface roughness. A qualitative and quantitative assessment of these factors has been presented in detail elsewhere (*11*, *44*). A brief discussion is given below.

**(a) Hydrodynamic Interaction.** Hydrodynamic interaction (resistance) of a spherical particle interacting with a planar surface depends on the diameter of the sphere and the distance of separation (*13–15*). An analysis of the effect of hydrodynamic interaction on the stability ratio (inverse of the attachment efficiency) in coagulation was carried out by Derjaguin and Muller (*48*) and Honig et al. (*49*). Their analysis showed that the effect of hydrodynamic interactions on the stability ratio is small and cannot account for the anomalous particle size effects. The theoretical stability curves obtained in this work are highly dependent on particle size, although hydrodynamic interactions were incorporated (partially) in the evaluation of $\alpha$. The effect of hydrodynamic interactions on the attachment efficiency in deposition of Brownian colloids is relatively small compared to that on non-Brownian particles (*50*). It is therefore concluded that hydrodynamic interactions cannot resolve the disparity with respect to particle size.

**(b) A Distribution in Surface Potential.** In the calculation of the theoretical attachment efficiencies it is assumed that the surface charge of particles and collectors is uniformly distributed, that all particles have a constant surface potential, and that all collectors also have a constant surface potential for a given solution chemistry. Electrophoretic mobility measurements of various colloidal particles indicate a wide distribution of mobility values (*51*). This indicates that individual particles in a suspension possess different values of surface potentials. Numerical calculations of the mean attachment efficiencies, assuming a normal distribution of surface potentials and collectors, were carried out in this work. The results show that a distribution of surface potentials can increase the theoretical attachment efficiencies and decrease the slopes of the $\log \alpha - \log C_s$ curves (*11*, *44*). However when these results are compared to the experimental stability curves, it is observed that the attachment efficiencies are still significantly smaller than the observed ones and that the slopes of the theoretical stability curves are much larger than those of the experimental curves.

**(c) Dynamics of Interaction.** Studies of interfacial electrodynamics (*52*, *53*) point out that it is possible, by considering the dynamics of interacting double layers, to provide some basis for the apparent insensitivity of colloidal stability to particle size. It was found that the extent of lateral adjustment of charge during interaction is dominated by hydrodynamic drag. Since the drag force depends on particle size, it may counteract the effect of the particle size on the rate of coagulation and deposition. However, no theory that treats rigorously the dynamics of interaction exists. The validity of the dependence of *static* forces on particle size, as observed in numerous adhesion studies (*54–56*), suggests that a better understanding of dynamics of interaction is important for resolving the disparity with respect to particle size.

**(d) Deposition in Secondary Minima.** Secondary minima in the total energy of interaction profile (based DLVO theory) can be obtained at moderate to large separation distances (usually larger than several nanometers). For given chemical conditions, the depth of the secondary minimum increases with particle size and the Hamaker constant of the interacting media. The apparent disparity with respect to particle size effects was observed in numerous coagulation studies (*25*, *57–60*). This discrepancy was attributed to deposition in primary and secondary minima. It was suggested that coagulation of larger particles in secondary minima is more pronounced since the depth of the secondary minima increases with particle size, and that this may counteract the decrease in the attachment efficiency with increasing particle size.

Significant deposition in secondary minima in the experimental system employed in this research is very unlikely. Theoretical analysis of the trajectory of a non-Brownian particle around a sphere in a creeping flow,

based on a force balance, predicts that collection in a secondary minimum is possible only in a small region at the rear stagnation point of the spherical collector (*2, 61, 62*). Similar predictions are expected for Brownian particles; particles trapped in a secondary mininum will translate and rotate due to fluid drag and shear until they reach the rear stagnation point where the net force (sum of van der Waals, electrical double layer, and fluid drag forces) on the particle is zero. Furthermore, the width of the secondary minimum region is of the order of a few nanometers, which implies that at most one particle can be collected by each collector.

**(e) Surface Roughness of Particles and Collectors.** The poor agreement between observations and theory in studies concerned with the kinetics of coagulation and deposition has been attributed to several factors. Among these factors is the surface roughness of particles and collectors. The disparity with respect to particle size was also attributed to surface roughness by Reerink and Overbeek (*57*). It was suggested that the total interaction energy may be determined by the radii of curvature of protrusions on surfaces rather than by the curvature of the interacting particles. Theoretical calculations considering static effects of surface roughness on the total interaction energy profile and on the attachment efficiencies were carried out (*11*). Protrusions on collectors were modeled as half spheres. The results show that such considerations can improve theoretical predictions. However, the discrepancies between theory and observations are not completely resolved. The effect of surface roughness on attachment efficiencies as discussed above is for *static* electrical double layer interaction theories. Surface roughness may also have a notable effect on interfacial dynamics of interaction (*52, 53*). The current understanding of dynamics of interaction is very poor and its effect on colloidal stability cannot be assessed quantitatively.

## *Summary and Conclusions*

A theoretical framework for chemical–colloidal effects on the kinetics of deposition of Brownian particles in porous media has been presented. The framework is formed by combining fundamental theories of particle transport, hydrodynamics, and colloidal stability (DLVO theory). A large sensitivity of the attachment efficiencies to the solution chemistry and surface potentials of colloids and collectors is predicted by theory. Theoretical computations also indicate that the slopes of the stability curves (log $\alpha$ – log $C_s$ curves) and the critical deposition concentrations depend on the particle size of the suspension.

Deposition experiments with suspensions of spherical latex colloids of various sizes and spherical glass bead collectors in packed-bed columns were conducted in order to test the theory. The results show that the experimental attachment efficiencies are orders of magnitude larger than the theoretical values. Attachment efficiencies were sensitive to the chemistry of the solution but not to the large extent predicted by theory. It was also found that the slopes of the experimental stability curves as well as the critical deposition concentrations are independent of particle size in a marked contrast to theoretical predictions.

It is most likely that these discrepancies are related to the failure of the DLVO theory to consider dynamics of interaction. Interfacial electrodynamics of interaction, coupling of electrodynamics and hydrodynamics, and the possible effects of surface roughness on dynamics of interaction are presumed to have a significant effect on the kinetics of particle–collector interactions. A better understanding of these processes is essential in order to resolve the discrepancies with respect to chemical–colloidal effects in the kinetics of particle deposition.

On the basis of the findings in this work, the attachment efficiency of colloidal particles in natural waters is expected to be independent of their particle size. This finding is of practical importance since colloidal particles in natural waters (e.g., hydrous oxides, clays, viruses, and organic macromolecules) are polydisperse and cover a wide size range (from several nanometers to a few micrometers). The solution chemistry of natural waters is not as simple as that used in this work. Dissolved organic and inorganic chemical species in natural waters are diverse and can affect markedly the stability of the particles. Thus, quantitative predictions of the kinetics of chemical–colloidal processes in natural waters with the framework of the DLVO theory is *not* feasible.

## *Literature Cited*


(1) Yao, K. M.; Habibian, M. T.; O'Melia, C. R. *Environ. Sci. Technol.* **1971**, *5*, 1105.
(2) Tien, C. *Granular Filtration of Aerosols and Hydrosols*; Butterworths Publishers: Stoneham, MA, 1989.
(3) Ghosh, M. M.; Jordan, T. A.; Porter, R. L. *J. Environ. Eng. Div. (Am. Soc. Civ. Eng.)* **1975**, *101*, 71.
(4) Rajagopalan, R.; Tien, C. *AIChE J.* **1976**, *22*, 523.
(5) Adamczyk, Z.; Zembla, M.; Siwek, B.; Czarnecki, J. *J. Colloid Interface Sci.* **1986**, *110*, 188.
(6) Adamczyk, Z. *Colloids Surf.* **1989**, *35*, 283.
(7) O'Melia, C. R. In *Aquatic Surface Chemistry*; Stumm, W., Ed.; Wiley-Interscience: New York, 1987.
(8) O'Melia, C. R. In *Aquatic Chemical Kinetics*; Stumm, W., Ed.; Wiley-Interscience: New York, in press.
(9) Tobiason, J. E.; O'Melia, C. R. *J.-Am. Water Works Assoc.* **1988**, *80*, 54.
(10) Ruckenstein, E.; Prieve, D. C. *J. Chem. Soc.*, Faraday *Trans. 2* **1973**, *69*, 1522.
(11) Elimelech, M. Ph.D. Dissertation; Johns Hopkins University, 1989.
(12) Spielman, L. A.; Friedlander, S. K. *J. Colloid Interface Sci.* **1974**, *46*, 22.
(13) Brenner, H. *Chem. Eng. Sci.* **1961**, *16*, 242.
(14) Goldman, A. J.; Cox, R. G.; Brenner, H. *Chem. Eng. Sci.* **1967**, *22*, 637.
(15) Goldman, A. J.; Cox, R. G.; Brenner, H. *Chem. Eng. Sci.* **1967**, *22*, 653.
(16) Dahneke, B. *J. Colloid Interface Sci.* **1974**, *48*, 520.
(17) Bird, R. B.; Stewart, W. E.; Lightfoot, E. N. *Transport Phenomena*; John Wiley & Sons: New York, 1960.
(18) Happel, J. *AIChE J.* **1958**, *4*, 197.
(19) Derjaguin, B. V.; Landau, L. D. *Acta Physicochim.* **1941**, *14*, 633.
(20) Verwey, E. J. W.; Overbeek, J. Th. G. *Theory of the Stability of Lyophobic Colloids*; Elsevier: Amsterdam, 1948.
(21) Nir, S. *Prog. Surf. Sci.* **1976**, *8*, 1.
(22) Gregory, J. *Adv. Colloid Interface Sci.* **1969**, *2*, 396.
(23) Gregory, J. *J. Colloid Interface Sci.* **1981**, *83*, 138.
(24) Hogg, R.; Healy, T. W.; Fuerstenau, D. W. *Trans. Faraday Soc.* **1966**, *62*, 1638.
(25) Wiese, G. R.; Healy, T. W. *Trans. Faraday Soc.* **1970**, *66*, 490.
(26) Friedlander, S. K. *Ind. Eng. Chem.* **1958**, *50*, 1161.
(27) Levich, V. G. *Physicochemical Hydrodynamics*; Prentice Hall: Englewood Cliffs, NJ, 1962.
(28) Van den Hul, H. J.; Vanderhoff, J. W. *J. Electroanal. Chem.* **1972**, *37*, 161.
(29) Stone-Masui, J.; Watillon, A. *J. Colloid Interface Sci.* **1975**, *52*, 479.
(30) James, R. O. In *Polymer Colloids*; Buscall, R., Corner, T., Stageman, J. F., Eds.; Elsevier: Amsterdam, 1985.
(31) Davis, J. A.; James, R. O.; Leckie, J. O. *J. Colloid Interface Sci.* **1978**, *63*, 480.
(32) Ottewill, R. H.; Shaw, J. N. *J. Electroanal. Chem.* **1972**, *37*, 133.
(33) Elimelech, M.; O'Melia, C. R. *Colloids Surf.* **1990**, *44*, 165.

(34) Habibian, M. T.; O'Melia, C. R. *J. Environ. Eng. Div. (Am. Soc. Civ. Eng.)* **1975**, *101*, 567.
(35) Yao, K. M. Ph.D. Dissertation; University of North Carolina at Chapel Hill, 1968.
(36) Spielman, L. A.; FitzPatrick, J. A. *J. Colloid Interface Sci.* **1973**, *42*, 607.
(37) Yoshimura, Y.: Ueda, K.; Mori, K.; Yoshoka, N. *Int. Chem. Eng.* **1980**, *20*, 600.
(38) Gregory, J.; Wishart, A. J. *Colloids Surf.* **1980**, *1*, 313.
(39) Hirtzel, C. J.; Rajagopalan, R. *Colloidal Phenomena*; Noyes Publications: Park Ridge, NJ, 1985.
(40) Adamczyk, Z.; Czarnecki, J.; Dabros, T.; van de Ven, T.G.M. *Adv. Colloid Interface Sci.* **1983**, *19*, 183.
(41) Wang, Z. Ph.D. Dissertation; Johns Hopkins University, 1985.
(42) Israelachvili, J. N. *Chem. Scr.* **1985**, *25*, 7.
(43) Elimelech, M. *J. Chem. Soc., Faraday Trans.* **1990**, *86*, 1623.
(44) Elimelech, M.; O'Melia C. R. *Langmuir* **1990**, *6*, 1153.
(45) Tobiason, J. E. *Colloids Surf.* **1989**, *39*, 53.
(46) Hull, M.; Kitchener, J. A. *Trans. Faraday Soc.* **1969**, *65*, 3093.
(47) Bowen, B. D.; Epstein, M. *J. Colloid Interface Sci.* **1979**, *72*, 81.
(48) Derjaguin, B. V.; Muller, V. M. *Dokl. Akad. Nauk SSSR (Engl. Transl.)* **1967**, *176*, 738.
(49) Honig, E. P.; Roebersen, G. J.; Wiersema, P. H. *J. Colloid Interface Sci.* **1971**, *36*, 97.
(50) Prieve, D. C.; Ruckenstein, E. *AIChE J.* **1974**, *20*, 1178.
(51) Rajagopalan, R.; Chu, R. Q. *J. Colloid Interface Sci.* **1982**, *86*, 299.
(52) Dukhin, S. S.; Lyklema, J. *Langmuir* **1987**, *3*, 94.
(53) Van Leeuwen, H. P.; Lyklema, J. *Ber. Bunsenges. Phys. Chem.* **1987**, *91*, 288.
(54) Tomlinson, G. A. *Philos. Mag. J. Sci.* **1928**, *6*, 695.
(55) Krupp, H. *Adv. Colloid Interface Sci.* **1967**, *1*, 111.
(56) Dahneke, B. *J. Colloid Interface Sci.* **1972**, *40*, 1.
(57) Reerink, H.; Overbeek, J. Th. G. *Discuss. Faraday Soc.* **1954**, *18*, 74.
(58) Ottewill, R. H.; Shaw, J. N. *Discuss. Faraday Soc.* **1966**, *42*, 154.
(59) Joseph-Petit, A. M.; Dumont, F.; Watillon, A. *J. Colloid Interface Sci.* **1973**, *43*, 649.
(60) Penners, N. H. G.; Koopal, L. K. *Colloids Surf.* **1987**, *28*, 67.
(61) Tobiason, J. E. Ph.D. Dissertation; Johns Hopkins University, 1987.
(62) Spielman, L. A.; Cukor, P. M. *J. Colloid Interface Sci.* **1973**, *43*, 51.

*Received for review March 12, 1990. Revised manuscript received June 1, 1990. Accepted June 20, 1990. We acknowledge the support of the U.S. Environmental Protection Agency under Research Grant R812760.*

# *N*-Chloramine Derivatization Mechanism with Dansylsulfinic Acid: Yields and Routes of Reaction

**James A. Jersey, E. Choshen, J. N. Jensen, and J. Donald Johnson***

Department of Environmental Sciences and Engineering, School of Public Health, University of North Carolina, Chapel Hill, North Carolina 27599-7400

**Frank E. Scully, Jr.**

Department of Chemical Sciences, Old Dominion University, Norfolk, Virginia 23508

■ At present, direct methods for analysis of chloramines are unavailable. Several approaches using derivatization-based methods for their anlaysis have been reported in the literature. One such method employs reaction of chloramines with dansylsulfinic acid to produce stable dansylsulfonamide products, which are analyzed by HPLC. This paper reports results of experiments examining the routes and yields produced during the dansylation of model chloramine solutions. Potential limitations of the method arise due to matrix effects, low yields for dilute chloramine concentrations, and a marked dependence of yield upon the composition of the chloramine pool. These limitations disallow quantitative application of the dansylation method to the analysis of chloramine mixtures.

## *Introduction*

When chlorine is used for water and wastewater disinfection, a wide variety of chloramines are formed (*1–3*). Some of these compounds may have important health implications (*4*). There is little data, however, on the composition and chemistry of the organic chloramine fraction in water or wastewater. To a large extent the gaps in our knowledge regarding the significance and environmental fate of the chloramines is due to the lack of sensitive and selective methods for their analysis.

Several researchers have proposed methods for analysis of chloramines that are based upon derivatization procedures and analysis of the resulting products by high-performance liquid chromatography (HPLC). The Scully et al. (*5*, *6*) method is based upon derivatization of chloramines with dansylsulfinic acid to produce stable and highly fluorescent dansylated products. Unfortunately this derivatization proceeds indirectly through the formation and reaction of the dansyl chloride intermediate. Lukasewycz et al. (*7*) proposed a derivatization method based upon 2-mercaptobenzothiazole. Although the yields are somewhat higher and the kinetics faster than the dansylation method, this derivatization procedure also appears to proceed through an intermediate and thus may suffer problems similar to those of the dansylation method discussed below.

Ammonia and glycine are both commonly found in wastewater (*8*) and upon chlorination are converted rapidly to their *N*-chloro derivatives (*9*). These compounds were selected as models for study of the routes and yields produced in derivatization of aqueous organic and inorganic chloramines with dansylsulfinic acid. The purpose of this paper is to clarify an assertion made in previous work of the dependence of product yields on relative kinetics (*5*). Specifically, kinetic and yield data from model compound solutions will be used to demonstrate limitations for quantitative application of the dansylation method to analysis of chloramine mixtures.

## *Experimental Section*

**Materials.** Amino acids and dansylated amino acid standards were obtained from Sigma Chemical Co. and used without further purification. Glassware contacting

 0013-936X/90/0924-1536$02.50/0 